Analysis of the morphometric variations in natural fibres by automated laser scanning: Towards an efficient and reliable assessment of the cross-sectional area

William Garat, Stéphane Corn, Nicolas Le Moigne, Johnny Beaugrand, Anne Bergeret

▶ **To cite this version:**

William Garat, Stéphane Corn, Nicolas Le Moigne, Johnny Beaugrand, Anne Bergeret. Analysis of the morphometric variations in natural fibres by automated laser scanning: Towards an efficient and reliable assessment of the cross-sectional area. Composites Part A: Applied Science and Manufacturing, 2018, 108, pp.114 - 123. 10.1016/j.compositesa.2018.02.018 . hal-01831128

HAL Id: hal-01831128
https://hal.science/hal-01831128v1

Submitted on 26 Jan 2021

HAL is a multi-disciplinary open access archive for the deposit and dissemination of scientific research documents, whether they are published or not. The documents may come from teaching and research institutions in France or abroad, or from public or private research centers.

L'archive ouverte pluridisciplinaire **HAL**, est destinée au dépôt et à la diffusion de documents scientifiques de niveau recherche, publiés ou non, émanant des établissements d'enseignement et de recherche français ou étrangers, des laboratoires publics ou privés.

Analysis of the morphometric variations in natural fibres by automated laser scanning: Towards an efficient and reliable assessment of the cross-sectional area

William Garat[a], Stephane Corn[a,*], Nicolas Le Moigne[a,*], Johnny Beaugrand[b,2], Anne Bergeret[a]

[a] C2MA, IMT Mines Ales, Université de Montpellier, 6 Avenue de Clavières, 30319 Ales Cedex, France[1]
[b] Fractionnement des Agro Ressources et Environnement (FARE), INRA, Université de Reims Champagne-Ardenne, 2 esplanade Roland Garros, F-51100 Reims, France

A B S T R A C T

The development of natural fibres in engineering applications requires the reliable and accurate assessment of their dimensional characteristics and mechanical properties. Fibre cross-sectional area (CSA) obtained from lateral dimensional measurements should consider the specific cross-sectional shape of natural fibres and its wide lengthwise morphometric variations. In this study, a detailed dimensional analysis was conducted on a selected panel of natural fibres with contrasted morphometric characteristics belonging to various phylogenetic plant species with dissimilar functions *in planta*. An automated laser scanning technique was used, and geometrical models and filtering data method were developed for calculation of reliable CSAs adapted to each plant fibre species. Results show that CSAs of palm and sisal fibre bundles can be satisfactorily assessed by a circular model with minimal data processing, whereas hemp, flax and nettle fibre bundles require specific data filtering due to partial splicing, and can be better assessed by an elliptic model.

Keywords:
A. Natural fibres
B. Optical properties/techniques
C. Statistical properties/methods
D. Optical microscopy
E. Morphometric analysis

1. Introduction

Composite industry shows growing interest in the development of biocomposites. Natural fibres of various botanical origins, such as hemp, flax or sisal, have been used as reinforcement in polymer composites [1–7] in substitution for glass fibres [8]. They offer a solution to current environmental issues, such as the reduction of greenhouse gas emissions and pollution, through the use of renewable and biodegradable resources for the development of lightweight materials [9]. However, natural fibres do not yet benefit from a sufficient scientific and technological background to offer a controlled and constant level of performances adapted to engineering applications as is the case of synthetic fibres [10–13]. In this regard, researchers, industrials and natural fibre producers investigate potential solutions to better control, model and predict the mechanical behaviour of biocomposites, by improving the extraction of technical natural fibres, the manufacturing of biocomposites and their conditions of service use [4]. This requires a thorough knowledge of the morphological characteristics of natural fibres, in particular their cross-sectional area (CSA) [14–20]. Indeed, the accuracy of the CSA measurements is crucial since the evaluation of the mechanical properties of natural fibres directly relies on the collected dimensional data and the data processing methods used to calculate their CSAs [21].

Several measurement methods based on Scanning Electron Microscopy (SEM) observations, optical microscopy and scanner measurements and observations of polished cross-section have been used to assess the dimensions of natural fibres [22–31]. Some authors [10,12,21,32,33] also related the measurement of the length, width and CSA of various natural fibre species with their mechanical properties. They evidenced wide variations both in terms of morphometric characteristics and resulting mechanical properties. However, several of these studies are based on simplified assumptions of the cross-sectional shape that could be valid for synthetic fibres but not for the specific shape and dimensional irregularities of natural fibres [10]. Indeed, in many cases, an assumption considering cross-section of natural fibres as circular and homogeneous is used, though natural fibres, whatever their botanical origin and the scale considered (i.e. elementary fibre cells or fibre bundles), show wide variations in their dimensional and morphometric features. Besides, their cross-sectional shape can vary from fibre to fibre and along their length [12,33–38]. This partly explains the large scattering in fibre mechanical properties reported in literature since many years [1,6,10,20]. Studying the tensile properties of flax

* Corresponding authors.
E-mail addresses: stephane.corn@mines-ales.fr (S. Corn), nicolas.le-moigne@mines-ales.fr (N. Le Moigne).
[1] C2MA is member of the European Polysaccharide Network of Excellence (EPNOE), http://www.epnoe.eu.
[2] Current address: Biopolymères Interactions Assemblages (BIA), INRA, Nantes, France.

fibre bundles, Haag and Müssig [21] proposed an advanced measurement technique of the CSA based on an automated laser scanning that has the advantage to measure the cross-sections dimensions all along the fibre and to be highly reproducible and not influenced by user. Nevertheless, the authors pointed out that errors can occur during laser measurements if partly spliced fibre bundles are measured instead of the whole element. They assume that filtering procedures can be necessary to exclude falsified data from the evaluation.

The purpose of this study is to develop a methodology to better assess the dimensional and morphometric characteristics of natural fibres from various botanical origin. Cross-sectional measurements obtained from optical microscopy observations are correlated with measurements recorded with an automated laser scanning technique. Based on these measurements, data processing approaches adapted to the morphometric characteristics of each plant fibre species are proposed for the reliable calculation of natural fibres CSAs.

2. Experimental section

2.1. Materials

The dimensional and morphometric analysis of natural fibres was conducted on fibre bundles from five different plant species, three of them belonging to Eudicots and are commonly called 'bast fiber', poorly lignified, with a support function of the stem *in planta*: flax (*Linum usitatissimum*) and hemp (*Canabis sativa*) as annual fibre crop (after retting step) and nettle (*Urtica dioica*) as an perennial herbaceous plant. The other two species are from perennial Monocots, highly lignified, with a dominant conducting tissues function *in planta*: sisal (*Agave sisalana*) coming from the leaf of agave and Palm (*Phoenix dactylifera*) are mats of leaf sheath surrounding the palm tree stems.

Due to either their various botanical origins and functions in plant (strength versus conducting), these fibre bundles are likely to show contrasted dimensional and morphometric characteristics as described in literature [4,10,39] and observed in Fig. 1. Wide variations in their cross-sectional dimensions as well as variations in their cross-sectional shape in terms of ellipticity and concavity are clearly observed.

2.2. Methods for the measurement of fibre bundle cross-section

2.2.1. Automated laser scanning measurements

For the automated laser scanning measurement, twelve fibre bundles of each plant species were cut to a length of roughly 3 mm. Then, each fibre bundle was positioned in a plastic tab before being fixed quickly (approximately 5 s) with a photo-curing glue (DYMAX, Wiesbaden, Germany). This step prevents fibre bundles from slipping out of the support due to gentle tension applied during measurements. Before automated laser scanning measurements, fibre bundles were conditioned at 23 °C and 50% RH overnight (12 h).

The automated laser scanning method used the Fibre Dimensional Analysis System (FDAS) device controlled by UvWin 3.60® software (Diastron Ltd., Hampshire, UK). This apparatus allows measuring apparent transverse dimensions of the fibre bundles with a resolution of 0.01 μm, thanks to a high accuracy non-contact laser measuring system (LSM 500S, Mitutoyo, Japan). Fibre bundles fixed on plastic tabs are maintained by a pneumatic system which allows 360° rotative scanning all along their length (Fig. 2a). For each scan position with a pitch of 40 μm along the fibre, up to 600 apparent diameters were measured on the rotating fibre bundle. This leads to more than 45.000 values of apparent diameter for a fibre bundle of 3 mm length. Then, apparent transverse dimensions such as maximum, minimum and average diameters can be deduced for each cross-section and along the fibre bundle (Fig. 2b). It should be pointed out that considering the measurement principle which is based on laser ombroscopy; concave surfaces cannot be measured with this device.

2.2.2. Optical microscopy measurements

Direct optical microscopy observations of the fibre bundles cross-sections were performed with a Leica Laborlux 12 POL S optical microscope in reflection mode equipped with a 1600 × 1200 pixels mono-CDD Sony digital camera. This method was used by Virk [25] for jute fibres, by Müssig et al. [10] and Thomason et al. [33] for flax and sisal fibres and by Navarro et al. [22] for less common plant fibre bundles. The fibre bundles analysed by the automated laser scanning technique beforehand were then embedded vertically in an epoxy resin-pad. The Geofix® resin (ESCIL, Chassieu, France) was used. It is a transparent resin specially formulated to impregnate samples (high fluidity and low shrinkage) with a curing time at room temperature of 24 h. Fibre

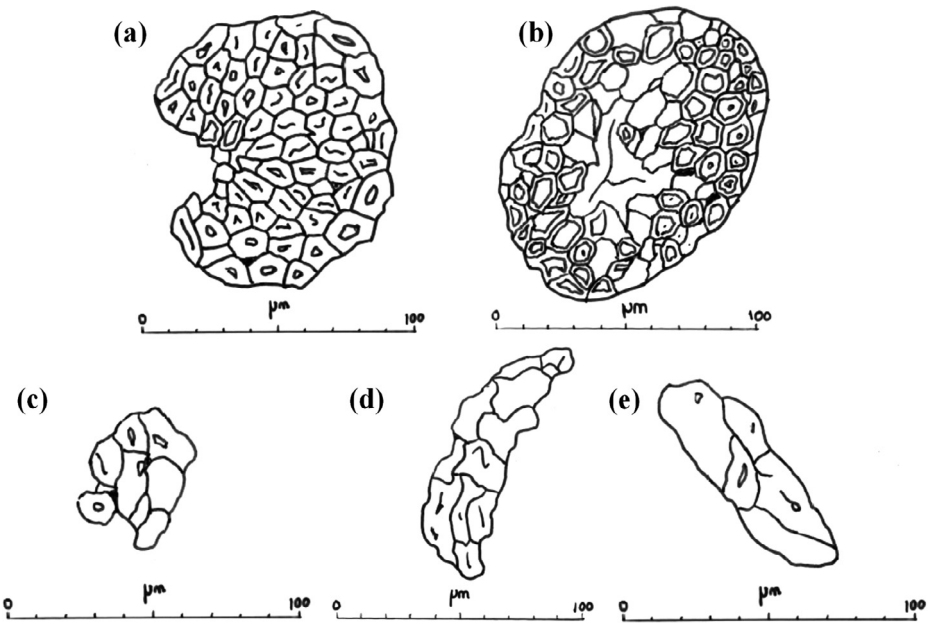

Fig. 1. Typical cross-sections of (a) sisal *Agave sisalana*, (b) palm *Phoenix dactylifera*, (c) flax *Linium usitatissimum*, (d) nettle *Urtica dioica*, and (e) hemp *Canabis sativa* drawn from optical microscopy observations.

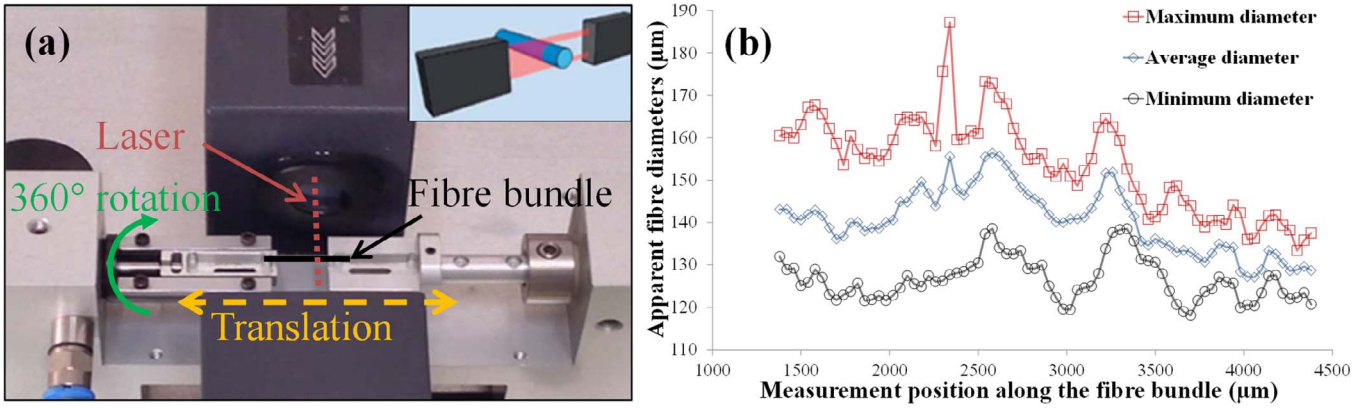

Fig. 2. (a) FDAS device principle and (b) minimum, maximum and average diameters along a palm fibre bundle as measured with the FDAS device.

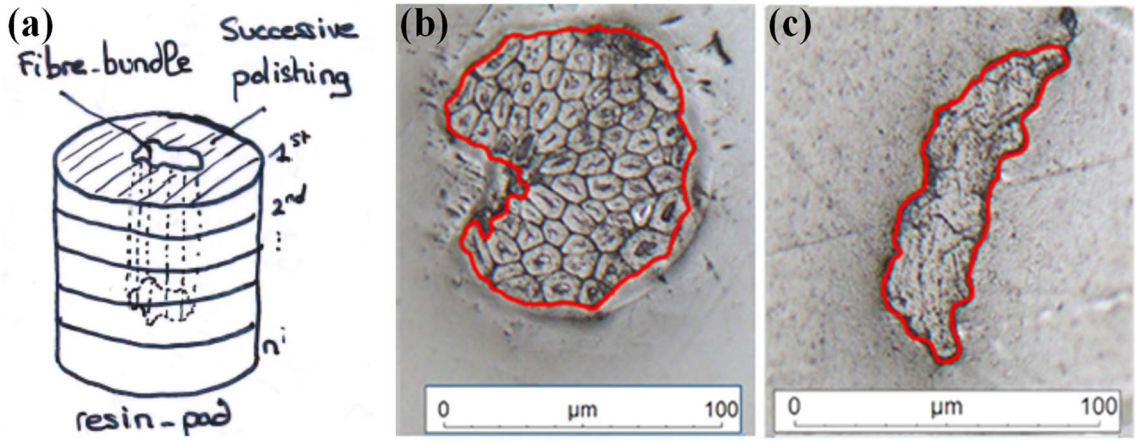

Fig. 3. (a) Scheme of an embedded fibre bundle in an epoxy resin-pad; Manual outline of the fibre bundle perimeter with the image processing software (Archimede®, Microvision Instruments, France) for (b) sisal and (c) nettle.

bundles axial position within the epoxy resin-pad was precisely determined so that the cross-sections measured by optical microscopy can be directly compared one to one with those measured by the automated laser scanning technique. The resin-pads containing the fibre bundles were gradually sanded with a pitch of roughly 300 µm. A ten-polishing sequences procedure using different fine polishing papers (600, 2400, 4000 grade) wetted with ethanol was achieved to ensure optimum observation quality (Fig. 3a). After each sanding and polishing step, the cross-section of each fibre bundle was observed under the optical microscope and their cross-sectional areas (CSA_{OM}) were measured with the image acquisition and processing software (Archimede®, Microvision Instruments, France). As shown in Fig. 3b and c, the outline of the fibre bundle cross-section was cropped manually to calculate its area. With 12 fibre bundle samples and 10 successive sanding and polishing sequences, this leads to approximately 120 CSA_{OM} measurements for each of the five plant species.

3. Results and discussion

3.1. Lengthwise morphometric variations in fibre bundles from various plant species

Based on the FDAS measurements, two main morphotypes among the five plant species were observed. Palm and sisal fibre bundles appear relatively uniform and regular with low intra-fibre variability, i.e. the minimum, maximum and average diameters are relatively constant along the fibre bundles (Fig. 4a). Moreover, the average diameter and maximum and minimum diameters are relatively close, suggesting that their cross-sectional shape is almost circular (Fig. 4b and c). Similar results were obtained for each fibre bundles samples from the same plant species, suggesting that, for the tested batch of sisal and palm fibre bundles, low inter-fibre bundles variability occurred. It should be pointed out that the cross-sections of sisal fibre bundles always showed a kidney shape which should be taken into account as the concave surfaces cannot be measured with the FDAS device (see Section 2.2.1.). Besides, palm and sisal fibre bundles are composed of many strongly packed elementary fibres, reported as highly lignified, with large lumen for some of them.

Flax, hemp and nettle fibre bundles are much more irregular with wide variations in the minimum, maximum and average diameters along their length, i.e. high intra-fibre variability (Fig. 5a). The large difference measured between their maximum and minimum diameters confirms their non-circularity, as can be evidently concluded from optical microscopy observations (Fig. 5b–d). Besides, the analysis of the whole data set available for flax, hemp and nettle fibre bundles showed that there is more inter-fibre bundles variability for these plant species. This has to be related to their botanical origin but also their harvesting and extraction conditions. In particular, the presence of elementary fibres detached from the main bundle was observed for retted flax fibres due to their lower intercellular cohesion that favoured fibre bundles splicing.

Based on these first observations, it is obvious that the simplifying geometrical assumption that considers natural fibre bundle cross-sections as being purely circular and uniform is not appropriate. In the following, a correlation between the data obtained from optical microscopy measurements and those measured by the automated laser scanning is carried on.

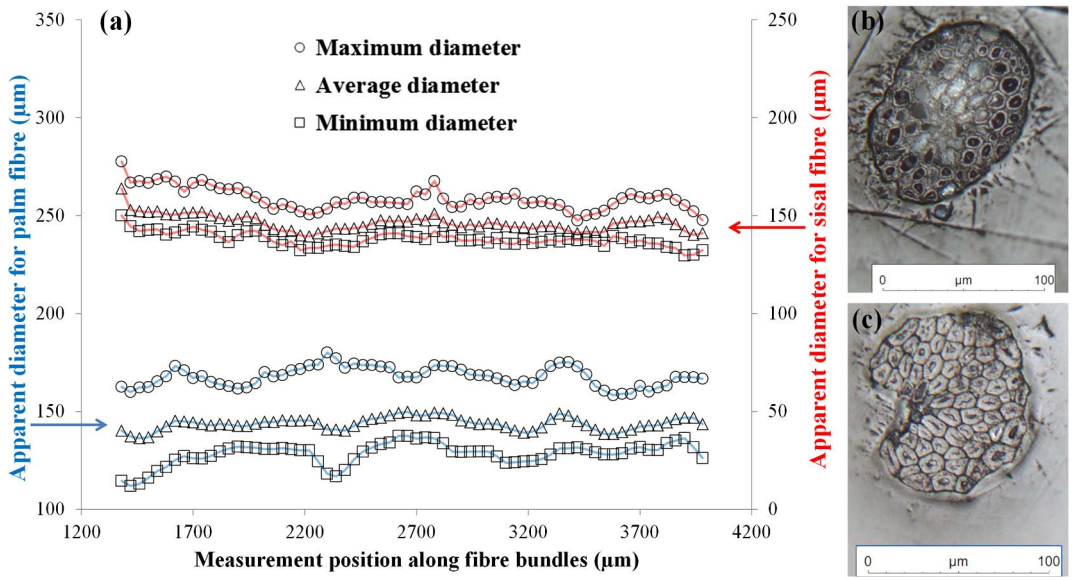

Fig. 4. (a) Lengthwise morphometric variations for palm and sisal fibre bundles from the FDAS, and typical cross-section of (b) palm and (c) sisal fibre bundles embedded in epoxy resin-pad as observed by optical microscopy.

3.2. Morphometric indicators of the (non-)circularity of natural fibre cross-section

Fig. 6 correlates the apparent median diameter D_{median} measured with the FDAS for each cross-sections of each fibre bundle sample and the CSA_{OM} of the corresponding cross-section (as determined by optical microscopy measurements). A data table gives the minimum, maximum and median apparent diameters and CSA_{OM} of the tested fibre bundles for the five plant species. For each plant species, the set of data pairs, i.e. CSA_{OM} from optical microscopy and corresponding D_{median} from FDAS, was fitted with a circular-like model by least squares method according to Equation 1:

$$CSA_{OM} = k \times D_{median}^2 \quad (1)$$

Where, k is an adjustable parameter that equals to $\pi/4$ (i.e. 0.785) for a perfect circular shape. The typical curve that should be obtained for a perfect circular shape was superimposed.

As seen in Table 1, a good correlation to the circular model was obtained for palm and sisal fibre bundles with k parameters equal to 0.778 and 0.702 respectively, very close to that of a perfect circular shape (0.785), and good coefficients of determination R^2 of 0.94 and 0.93 respectively. For the other plant species, k parameters were much lower, 0.605, 0.660 and 0.485 for hemp, flax and nettle fibre bundles, respectively, suggesting a strong deviation to the circular shape for these fibre bundles. Larger scattering to the best fit obtained with k was also observed with coefficients of determination R^2 of 0.88, 0.68 and 0.79, respectively. It should be pointed out that deviations to the circular model do not seem to be diameter dependent because there is substantial overlapping of apparent median diameter values between the different plant species considered in this study.

To complete this first approach and determine if morphometric indicators can be attributed to each plant fibre species, shape factors α were calculated based on the ratio of the maximum to the minimum diameters obtained by FDAS measurement for each fibre bundle cross-section of the different plant species (Equation 2):

$$\alpha = \frac{D_{max}}{D_{min}} \quad (2)$$

Exhibiting median shape factors of 1.17 and 1.24, respectively, cross-sectional shapes of palm and sisal fibre bundles appear to be close to a circular shape (Fig. 7). In contrast, hemp, flax and nettle fibre bundles present median shape factors of 2.35, 2.58 and 2.74, respectively, with a wider dispersion. These results are in agreement with previous observations and conclusions made from the results presented in Fig. 5 and Fig. 6, and suggest that a geometrical model based on the assumption of an elliptical cross-sectional shape would be more suitable for the calculation of CSAs for hemp, flax and nettle fibre bundles. Furthermore, the determination of shape factors from FDAS measurements appears as an easy-to-calculate and robust morphometric indicator to assess the circularity of cross-sections in natural fibre bundles, whatever the diameter considered (Fig. 6).

3.3. Geometrical models and filtering method for the determination of CSAs in natural fibre bundles

Several studies have been conducted on natural fibre dimensional measurements, i.e. diameters and sections. Many studies considered natural fibres as circular and regular objects [25,40]. This hypothesis does not take into account the non-circularity of the fibre cross-section, neither does the variability of the fibre cross-section along their length [12]. Other authors took into account the irregularity of the section and considered the cross-section as elliptic [12,21], hexagonal [41] or as a convex hull [42], to better assess the real cross-sectional shape of natural fibres. It should be pointed out that all these assumptions on the cross-sectional shape of the fibres directly influence the evaluation of their mechanical properties and can contribute to the large scattering found in literature for tensile strength and elastic modulus of natural fibres.

Because of the considerable number of apparent diameter values that can be collected in a reasonable time, the use of an automated laser scanning device appears as a relevant and robust method which should allow taking into account apparent dimensional irregularities of natural fibre bundles. Based on the morphometric analysis, two morphotypes have been identified: (i) palm and sisal fibre bundles which present a lengthwise regular cross-sectional shape and low shape factors close to 1, and (ii) hemp, flax and nettle fibre bundles which present wide lengthwise dimensional variations as well as irregular cross-sectional shapes with high shape factors up to 2.74. According to these morphometric features, different approaches of data processing and geometrical models were applied to FDAS data for CSA calculation as shown in Table 2.

The simplest approach is the circular model (Eq. (3)) which considers the apparent median diameter of each cross-section, determined

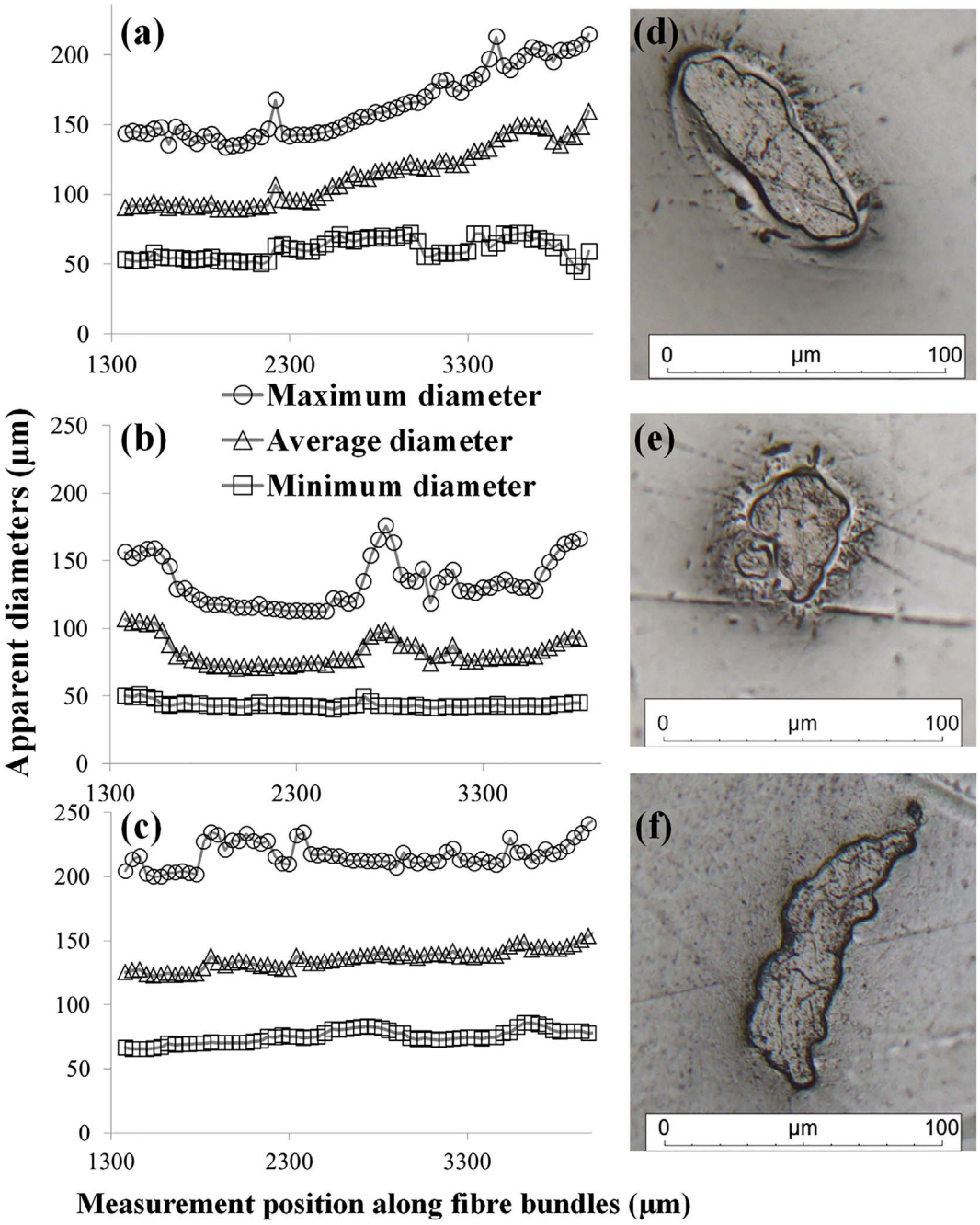

Fig. 5. Lengthwise morphometric variations (minimum, maximum and average diameters) for (a) hemp, (b) flax and (c) nettle fibre bundles, and typical cross-section of (d) hemp, (e) flax and (f) nettle fibre bundles embedded in epoxy resin-pad as observed by optical microscopy.

from 600 diameter values, to calculate the CSA. It is valid for fibre bundles having a nearly circular cross-sectional shape. The elliptic model (Eq. (4)) uses the maximum and minimum apparent diameters of each cross-section, extracted from 600 values, to calculate the CSA. The filtered elliptic model (Eq. (5)) has been developed in this work to exclude wrong data obtained with FDAS device, due to partly spliced fibre bundles with detached elementary fibres (Fig. 8a) that can greatly mislead the determination of the maximum and minimum diameters. This model is based on a statistical approach that considers the occurrence frequency of apparent diameters during the data acquisition. As shown in Fig. 8 for the scan of a flax fibre bundle cross-section, the presence of detached elementary fibres can be identified by the appearance of peaks of low frequency (< 0.5%), generally located at small diameter range of the order of the elementary fibre cell (Fig. 8b). It is then possible to identify, for each cross-section scan, the wrong values and exclude them from the statistical dataset. Filtered minimum D'_{min} and maximum D'_{max} diameters can be identified and used for the calculation of the CSA (Eq. (5)).

The three methods of data processing described in Table 2 to determine CSA from FDAS measurements were applied to the five plant fibre species, and the resulting CSA_{FDAS} were compared to the CSA_{OM} measured by optical microscopy.

3.3.1. Natural fibres with regular cross-sectional shape and low shape factor

Fig. 9 shows a radar graph of the apparent diameters obtained from FDAS measurements for one specific cross-section of a palm (a) and sisal (b) fibre bundle. For palm, the radar pattern appears relatively

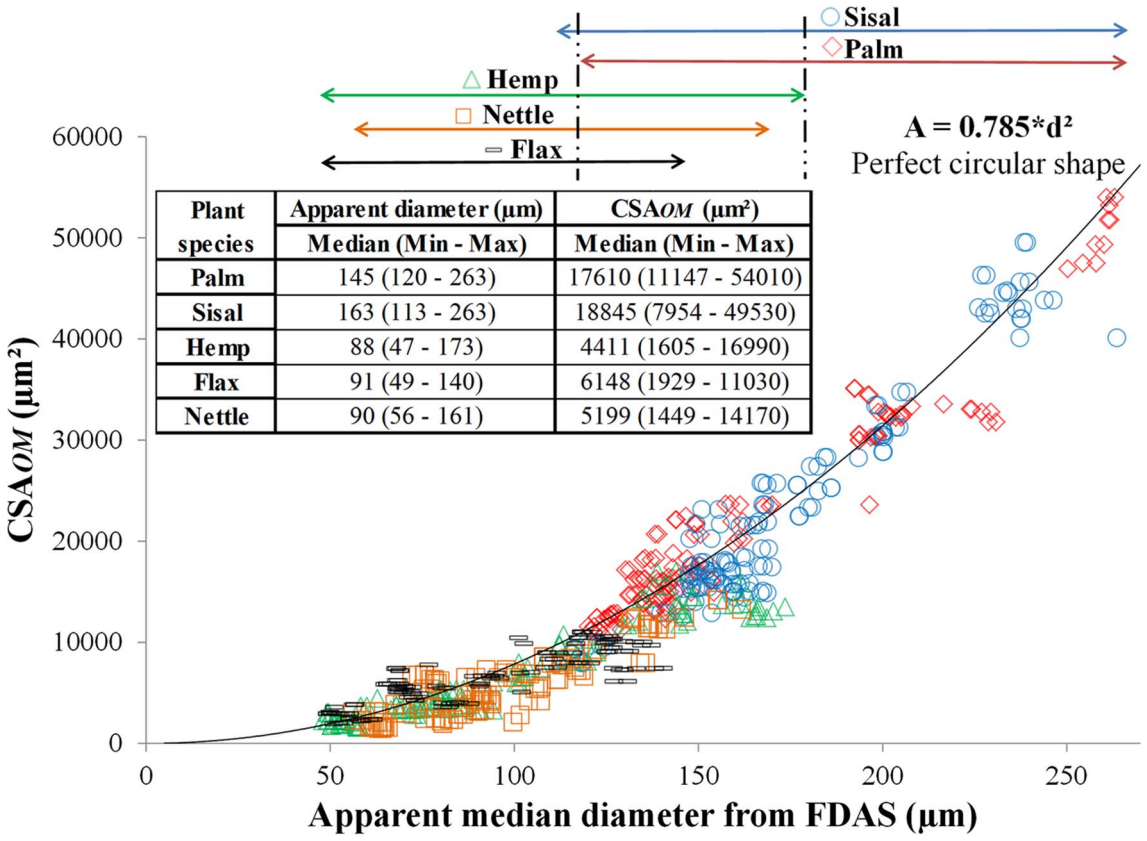

Plant species	Apparent diameter (µm) Median (Min - Max)	CSA*OM* (µm²) Median (Min - Max)
Palm	145 (120 - 263)	17610 (11147 - 54010)
Sisal	163 (113 - 263)	18845 (7954 - 49530)
Hemp	88 (47 - 173)	4411 (1605 - 16990)
Flax	91 (49 - 140)	6148 (1929 - 11030)
Nettle	90 (56 - 161)	5199 (1449 - 14170)

Fig. 6. Correlation between CSA_{OM} measured by optical microscopy and corresponding apparent median diameters (D_{median}) measured by FDAS for sisal, palm, hemp, nettle and flax fibre bundles. (Full line corresponds to the curve obtained for a perfect circular shape).

Table 1
Fibre cross-sectional shape analysis based on a circular model.

Fibre bundles	Number of data pairs (CSA_{OM} – D_{median})	k	R^2
Perfect cylinder	–	0.785	1
Palm	140	0.778	0.94
Sisal	138	0.702	0.93
Hemp	125	0.605	0.88
Flax	130	0.660	0.68
Nettle	120	0.485	0.79

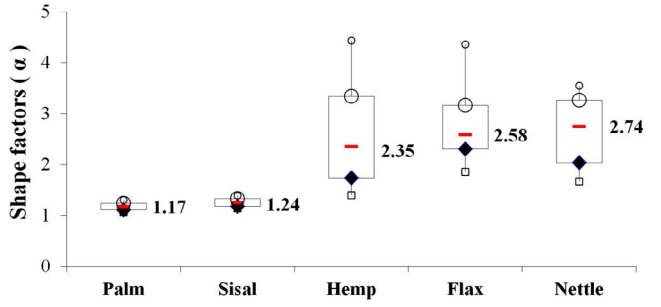

Fig. 7. Boxplots of fibre bundles shape factors α for the different plant species (palm, sisal, hemp, flax, nettle).

Table 2
Geometrical models and data processing approaches used to calculate the CSA from FDAS measurements.

Method	Geometric representation	Calculation formula
Circular model	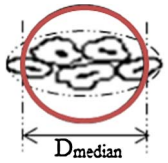	$CSA = \frac{\pi}{4} \times D_{median}^2$ (Eq. (3))
Elliptic model	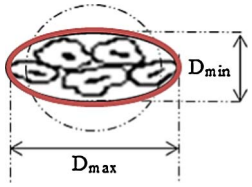	$CSA = \frac{\pi}{4} \times D_{min} \times D_{max}$ (Eq. (4))
Filtered elliptic model	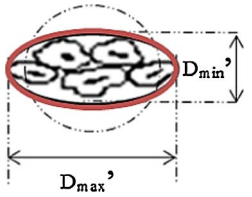	$CSA = \frac{\pi}{4} \times D'_{min} \times D'_{max}$ (Eq. (5))

circular, with a low deviation to the three models, and CSA_{OM} is very close to CSAs obtained from the models (23,460 µm² versus 25,522 µm² and 23,297 µm² for circular and elliptic models, respectively). For sisal, the deviation is slightly increased because of its particular kidney shape cross-section (Fig. 1a).

Considering now the whole data set, a good correlation was found between CSA_{OM} and CSA_{FDAS} values for palm fibre bundles (Fig. 10a), whatever the model used, with coefficients of determination higher than 0.95. Moreover, the correction factor C defined by $CSA_{FDAS} = C \times CSA_{OM}$ was close to 1, attesting for a very good estimation of the CSA with the automated laser scanning method.

For sisal fibre bundles (Fig. 10b), only slight differences between the three models are observed. Coefficients of determination are roughly

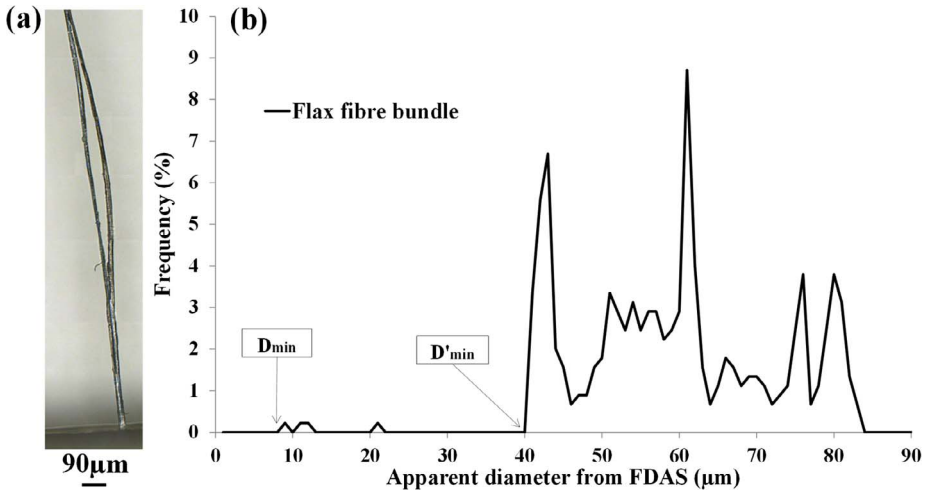

Fig. 8. (a) Optical micrograph of a flax fibre bundle with a detached elementary fibre, (b) corresponding occurrence frequency of diameters (interval unit: 1 µm) for one cross-section scan.

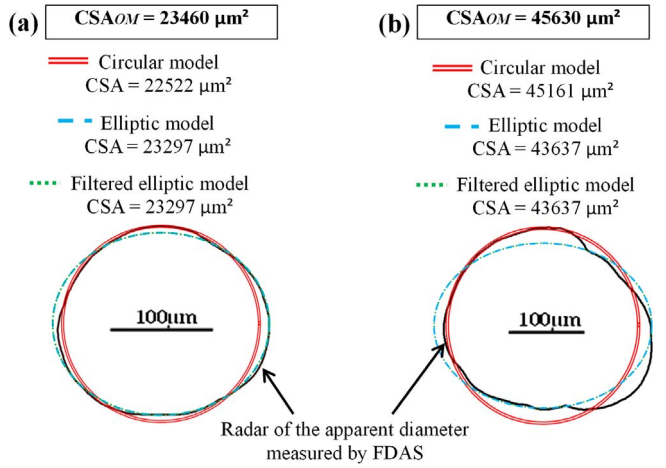

Fig. 9. Radar of the apparent diameters from FDAS and corresponding modelled cross-sections for one palm (a) and sisal (b) fibre bundle cross-section.

0.9, and the analysis of correction factors *C* showed that the circular model slightly overestimates CSA_{OM} with a *C* value of 1.02, whereas both elliptical models slightly underestimate CSA_{OM} with a *C* value of 0.97. The kidney shape of sisal fibre bundles and the resulting concave surfaces do not seem to hamper the reliable and accurate determination of their CSA.

Our results thus show that CSAs of regular palm and sisal fibre bundles can be satisfactorily approached from the FDAS measurements using a circular model with minimal data processing. Indeed, the filtered elliptic model does not enhance accuracy since the intercellular cohesion within the fibre bundles is sufficient to avoid any fibre bundle splicing. It should be pointed out that no fibre sample pre-treatments aiming at fibre individualization were used for sisal or palm fibre bundles. Also, both bundles are reported to be highly cohesive thanks to a high lignin amount, arguably in their middle lamellas.

3.3.2. Natural fibres with irregular cross-sectional shape and high shape factor

For hemp, flax and nettle fibre bundles, an important deviation from circularity characterised by high shape factors was found (Fig. 7). Moreover, large lengthwise morphometric variations were highlighted.

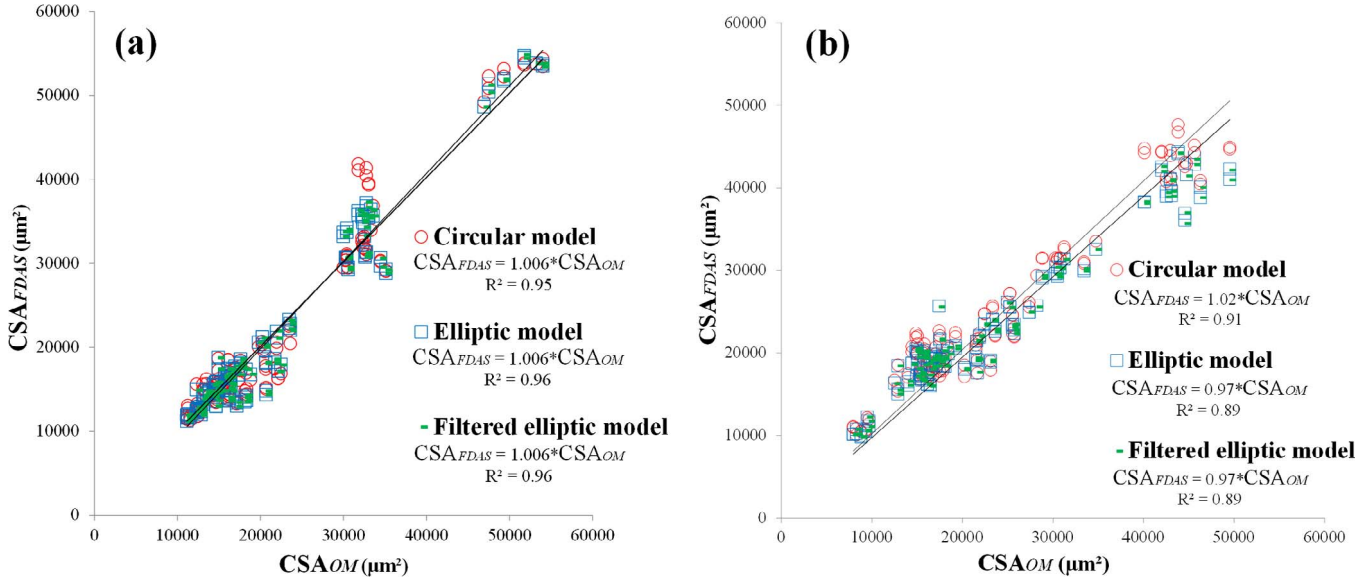

Fig. 10. Correlation between CSA_{FDAS} and CSA_{OM} for circular, elliptic and filtered elliptic models for (a) palm and (b) sisal fibre bundles.

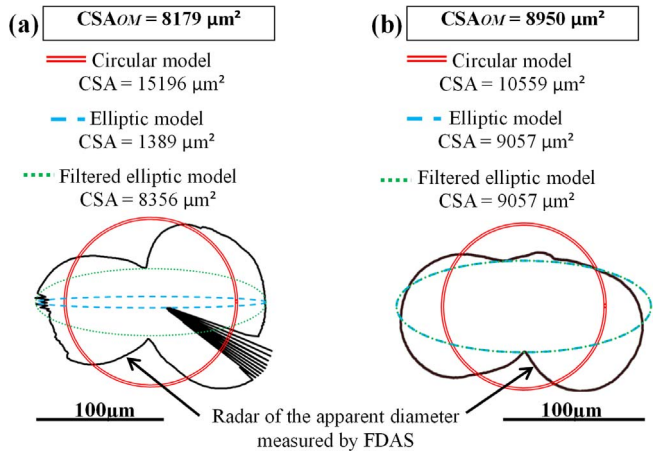

Fig. 11. Radar of the apparent diameters from FDAS and corresponding modelled cross-sections for one flax fibre bundle cross-section, (a) with fibre bundle splicing, and (b) without fibre bundle splicing.

In this regard, the use of an elliptical model appears more appropriate to determine the CSA.

Fig. 11 shows the radar of the apparent diameter obtained from FDAS measurements for one flax cross-section with fibre bundle splicing and one without. In both cases, the radar patterns are close to that of an ellipse. In the absence of measurement defects, the elliptic model is appropriate with CSA of 9057 µm^2 compared to CSA$_{OM}$ of 8950 µm^2 (Fig. 11b). On the other hand, the use of a filtered elliptic model is mandatory to identify and eliminate wrong apparent diameter values, responsible for the large deviation of the simple elliptic model as evidenced in Fig. 11a with a large error in the CSA determination (1389 µm^2 versus 8179 µm^2 for the CSA$_{OM}$).

Considering the whole data set for hemp and flax fibre bundles (Fig. 12a and b), the circular model gives higher coefficients of determination. However, this model significantly overestimates the CSA. For nettle fibre bundles (Fig. 12c), the elliptic model is better with a slightly higher coefficient of determination and a correction factor C of 1.01.

For all these fibre bundles, the filtered elliptic model appears to greatly enhance the quality of the correlation with CSA_{OM}. Coefficients of determination are indeed greatly increased and correction factors are closer to 1. This is explained by the numerous splicing of fibre bundles related to lower intercellular cohesion, that produce wrong data for these plant fibres, especially low apparent diameter values originating from detached elementary fibres. These wrong data must be excluded from the analysis, and the filtered elliptic model developed in this study greatly enhances the determination of the CSA for the irregular cross-

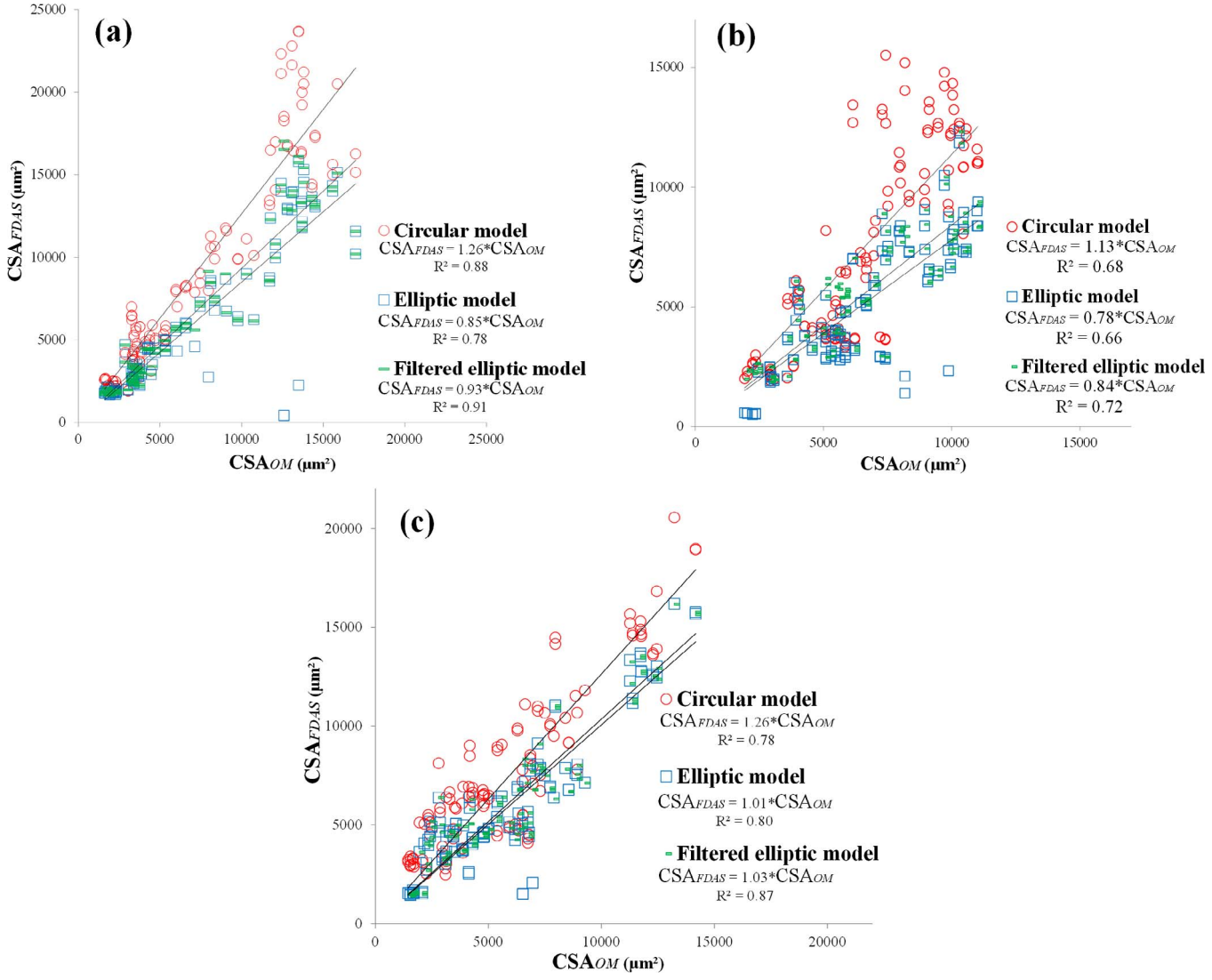

Fig. 12. Correlation between CSA_{FDAS} and CSA_{OM} for circular, elliptic and filtered elliptic models for (a) hemp, (b) flax and (c) nettle fibre bundles.

sectional shapes encountered in natural fibres. This filtering method can be implemented in routine as an automated post-processing of the data obtained from the laser scanning method.

4. Conclusions

The morphometric variations occurring in natural fibres have been investigated. Various plant fibre species (sisal, palm, flax, hemp, and nettle) having contrasted morphometric characteristics were analysed by optical microscopy and automated laser scanning (FDAS) measurements. Two main morphotypes have been identified: (i) monocots palm and sisal fibre bundles from leaves which presented a lengthwise regular cross-sectional shape and low shape factor close to 1, and in contrast (ii) eudicots hemp, flax and nettle fibre bundles from bast fibres which presented wide lengthwise dimensional variations as well as irregular cross-sectional shape and high shape factors up to 2.74. Based on these observations, geometrical models and a filtering method were applied to the FDAS data so as to determine the best approach to calculate the cross-sectional area (CSA) of each plant fibre species. Our results show that CSAs of regular palm and sisal fibre bundles can be satisfactorily assessed from the FDAS measurements using a circular model with minimal data processing. For more irregular cross-sectional shape encountered in natural fibres such as hemp, flax and nettle, the filtered elliptic model developed in the present study greatly enhances the determination of the CSA. This filtering method can be implemented in routine as an automated post-processing of the data obtained from the FDAS. Furthermore, based on the CSA measured by optical microscopy, CSA correction factors were determined for each plant fibre species and the applied geometrical models so that an accurate CSA can be calculated from the automated laser scanning data. The methodology developed in this study appears as a fast, efficient and reliable approach for the assessment of the cross-sectional area in natural fibres. This opens interesting perspectives for a better assessment of natural fibre tensile properties both for research and quality control purposes in industry.

Acknowledgements

William Garat thanks Montpellier SupAgro for funding its thesis scholarship. The authors thank Alain Diaz (IMT Mines Ales, C2MA) for technical support on the preparation of the samples, Arnaud Day (Fibres Recherche Développement, Troyes, France) for providing the nettle fibres and Yann Leray and Steve Bucknell (Diastron Ltd., Hampshire, UK) for technical support on FDAS device.

References

[1] Bledzki A, Gassan J. Composites reinforced with cellulose based fibres. Prog Polym Sci 1999;24:221–74. http://dx.doi.org/10.1016/S0079-6700(98)00018-5.
[2] Joshi SV, Drzal LT, Mohanty AK, Arora S. Are natural fiber composites environmentally superior to glass fiber reinforced composites? Compos Part A Appl Sci Manuf 2004;35:371–6. http://dx.doi.org/10.1016/j.compositesa.2003.09.016.
[3] Mohanty A, Misra M, Drzal L. Natural fiber bioplymers and biocomposites. Taylor & Francis; 2005.
[4] Baley C. Fibres naturelles de renfort pour matériaux composites. Technique de L'ingénieur. N 2 220; 2005. p. 1–12.
[5] Goda K, Cao Y. Research and development of fully green composites reinforced with natural fibers. J Solid Mech Mater Eng 2007;1:1073–84. http://dx.doi.org/10.1299/jmmp.1.1073.
[6] Faruk O, Bledzki AK, Fink H-P, Sain M. Biocomposites reinforced with natural fibers: 2000–2010. Prog Polym Sci 2012;37:1552–96. http://dx.doi.org/10.1016/j.progpolymsci.2012.04.003.
[7] Yan L, Chouw N, Jayaraman K. Flax fibre and its composites – a review. Compos Part B Eng 2014;56:296–317. http://dx.doi.org/10.1016/j.compositesb.2013.08.014.
[8] Wambua P, Ivens J, Verpoest I. Natural fibres: can they replace glass in fibre reinforced plastics? Compos Sci Technol 2003;63:1259–64. http://dx.doi.org/10.1016/S0266-3538(03)00096-4.
[9] Mohanty AK, Misra M, Drzal LT. Sustainable bio-composites from renewable resources: opportunities and challenges in the green materials world. J Polym Environ 2002;10:19–26.
[10] Müssig J, Fischer H, Graupner N, Drieling A. Testing methods for measuring physical and mechanical fibre properties (plant and animal fibres). Ind. Appl. Nat. Fibres. Chichester (UK): John Wiley & Sons, Ltd; 2010. p. 267–309. doi: 10.1002/9780470660324.ch13.
[11] Thuault A, Eve S, Blond D, Bréard J, Gomina M. Effects of the hygrothermal environment on the mechanical properties of flax fibres. J Compos Mater 2014;48:1699–707. http://dx.doi.org/10.1177/0021998313490217.
[12] Thomason JL, Carruthers J, Kelly J, Johnson G. Fibre cross-section determination and variability in sisal and flax and its effects on fibre performance characterisation. Compos Sci Technol 2011;71:1008–15. http://dx.doi.org/10.1016/j.compscitech.2011.03.007.
[13] Haag K, Padovani J, Fita S, Trouvé JP, Pineau C, Hawkins S, et al. Influence of flax fibre variety and year-to-year variability on composite properties. Ind Crops Prod 2017;98:1–9. http://dx.doi.org/10.1016/j.indcrop.2016.12.028.
[14] Bourmaud A, Gibaud M, Baley C. Impact of the seeding rate on flax stem stability and the mechanical properties of elementary fibres. Ind Crops Prod 2016;80:17–25. http://dx.doi.org/10.1016/j.indcrop.2015.10.053.
[15] Stamboulis A, Baillie CA, Peijs T. Effects of environmental conditions on mechanical and physical properties of flax fibers. Compos Part A Appl Sci Manuf 2001;32:1105–15. http://dx.doi.org/10.1016/S1359-835X(01)00032-X.
[16] Placet V, Cisse O, Boubakar ML. Influence of environmental relative humidity on the tensile and rotational behaviour of hemp fibres. J Mater Sci 2012;47:3435–46. http://dx.doi.org/10.1007/s10853-011-6191-3.
[17] De Rosa IM, Kenny JM, Puglia D, Santulli C, Sarasini F. Morphological, thermal and mechanical characterization of okra (Abelmoschus esculentus) fibres as potential reinforcement in polymer composites. Compos Sci Technol 2010;70:116–22. http://dx.doi.org/10.1016/j.compscitech.2009.09.013.
[18] Hidalgo-Reyes M, Caballero-Caballero M, HernáNdez-Gómez LH, Urriolagoitia-Calderón G. Chemical and morphological characterization of Agave angustifolia bagasse fibers. Bot Sci 2015;93:807–17. http://dx.doi.org/10.17129/botsci.250.
[19] Lanzilao G, Goswami P, Blackburn RS. Study of the morphological characteristics and physical properties of Himalayan giant nettle (Girardinia diversifolia L.) fibre in comparison with European nettle (Urtica dioica L.) fibre. Mater Lett 2016;181:200–3. http://dx.doi.org/10.1016/j.matlet.2016.06.044.
[20] Shah DU, Nag RK, Clifford MJ. Why do we observe significant differences between measured and "back-calculated" properties of natural fibres? Cellulose 2016;23:1481–90. http://dx.doi.org/10.1007/s10570-016-0926-x.
[21] Haag K, Müssig J. Scatter in tensile properties of flax fibre bundles: influence of determination and calculation of the cross-sectional area. J Mater Sci 2016;51:7907–17. http://dx.doi.org/10.1007/s10853-016-0052-z.
[22] Navarro CIT, Paciornik S, D'Almeida JRM. Microstructural characterization of natural fibers: etlingera elatior, costus comosus, and heliconia bihai. Conf Pap Mater Sci 2013;2013:1–7. http://dx.doi.org/10.1155/2013/878014.
[23] Romão C, Vieira P, Peito F, Marques AT, Esteves JL. Single filament mechanical characterisation of hemp fibres for reinforcing composite materials. Mol Cryst Liq Cryst 2004;418:87–99. http://dx.doi.org/10.1080/15421400490479172.
[24] Ilczyszyn F, Cherouat A, Montay G. Effect of hemp fibre morphology on the mechanical properties of vegetal fibre composite material. Adv Mater Res 2014;875–877:485–9. http://dx.doi.org/10.4028/www.scientific.net/AMR.875-877.485.
[25] Virk AS. Numerical models for natural fibre composites with stochastic properties. Doctoral dissertation Plymouth University; 2010. Available at https://pearl.plymouth.ac.uk/handle/10026.1/517.
[26] Thuault A, Eve S, Bazin J, Charlet K, Destaing F, Gomina M, et al. Morphologie, biocomposition et comportement mécanique des fibres de lin. Matériaux Tech 2011;99:275–80. http://dx.doi.org/10.1051/mattech/2011011.
[27] Grishanov SA, Harwood RJ, Booth I. A method of estimating the single flax fibre fineness using data from the LaserScan system. Ind Crops Prod 2006;23:273–87. http://dx.doi.org/10.1016/j.indcrop.2005.08.003.
[28] Mwaikambo LY, Ansell MP. Mechanical properties of alkali treated plant fibres and their potential as reinforcement materials. I. hemp fibres. J Mater Sci 2006;41:2483–96. http://dx.doi.org/10.1007/s10853-006-5098-x.
[29] Mwaikambo LY, Ansell MP. The effect of chemical treatment on the properties of hemp, sisal, jute and kapok for composite reinforcement. Die Angew Makromol Chem 1999;272:108–16. http://dx.doi.org/10.1002/(SICI)1522-9505(19991201)272:1**108::AID-APMC108>3.0.CO;2-9.
[30] Alves Fidelis ME, Pereira TVC, Gomes O da FM, de Andrade Silva F, Toledo Filho RD. The effect of fiber morphology on the tensile strength of natural fibers. J Mater Res Technol 2013;2:149–57. http://dx.doi.org/10.1016/j.jmrt.2013.02.00.
[31] d'Almeida J, Mauricio M, Paciornik S. Evaluation of the cross-section of lignocellulosic fibers using digital microscopy and image analysis. J Compos Mater 2012;46:3057–65. http://dx.doi.org/10.1177/0021998311435532.
[32] Charlet K, Jernot JP, Eve S, Gomina M, Bréard J. Multi-scale morphological characterisation of flax: from the stem to the fibrils. Carbohydr Polym 2010;82:54–61. http://dx.doi.org/10.1016/j.carbpol.2010.04.022.
[33] Thomason JL, Carruthers J. Natural fibre cross sectional area, its variability and effects on the determination of fibre properties. J Biobased Mater Bioenergy 2012;6:424–30. http://dx.doi.org/10.1166/jbmb.2012.1231.
[34] Munawar S, Umemura K, Kawai S, Sofyan Munawar S, Umemura K, Kawai S. Characterization of the morphological, physical, and mechanical properties of seven nonwood plant fiber bundles. J Wood Sci 2007;53:108–13. http://dx.doi.org/10.1007/s10086-006-0836-x.
[35] da Costa LL, Loiola RL, Monteiro SN. Diameter dependence of tensile strength by Weibull analysis: Part I bamboo fiber. Matéria (Rio Janeiro) 2010;15:110–6. http://dx.doi.org/10.1590/S1517-70762010000200004.
[36] Bevitori AB, Da SilvaA, Lopes FPD, Monteiro SN. Diameter dependence of tensile

strength by Weibull analysis: Part II jute fiber. Matéria (Rio Janeiro) 2010;15:117–23. http://dx.doi.org/10.1590/S1517-70762010000200005.
[37] Inacio WP, Lopes FPD, Monteiro SN. Diameter dependence of tensile strength by Weibull analysis: Part III sisal fiber. Matéria (Rio Janeiro) 2010;15:124–30. http://dx.doi.org/10.1590/S1517-70762010000200006.
[38] Charlet K, Baley C, Morvan C, Jernot JP, Gomina M, Bréard J. Characteristics of Hermès flax fibres as a function of their location in the stem and properties of the derived unidirectional composites. Compos Part A Appl Sci Manuf 2007;38:1912–21. http://dx.doi.org/10.1016/j.compositesa.2007.03.006.
[39] Bourmaud A, Dhakal H, Habrant A, Padovani J, Siniscalco D, Ramage MH, et al. Exploring the potential of waste leaf sheath date palm fibres for composite reinforcement through a structural and mechanical analysis. Compos Part A Appl Sci Manuf 2017;103:292–303. http://dx.doi.org/10.1016/J.COMPOSITESA.2017.10.017.
[40] Wang HH, Drummond JG, Reath SM, Hunt K, Watson PA. An improved fibril angle measurement method for wood fibres. Wood Sci Technol 2001;34:493–503. http://dx.doi.org/10.1007/s002260000068.
[41] Nitta Y, Goda K, Noda J, Lee W. Il. Cross-sectional area evaluation and tensile properties of alkali-treated kenaf fibres. Compos Part A Appl Sci Manuf 2013;49:132–8. http://dx.doi.org/10.1016/j.compositesa.2013.02.003.
[42] Virk AS, Hall W, Summerscales J. Physical characterization of jute technical fibers: fiber dimensions. J Nat Fibers 2010;7:216–28. http://dx.doi.org/10.1080/15440478.2010.504389.